Simulation of Unstable Crack Propagation by a Two-Dimensional Dynamic Linear Elastic Finite Element Computer Program

C. Lusso, C. Sampietri
CISE S.p.A., C.P. 12081, I-20134 Milano, Italy
P.P. Milella
ENEA, Via Brancati 48, I-00100 Roma, Italy

Abstract

A finite element bi-dimensional linear elastic computer code is presented. The code, called SPACCA, simulates the propagation and arrest of unstable cracks knowing either the crack propagation speed or the dynamic energy release rate $G_D(\dot{a})$ of the material.

Several options are available as to the force relaxation modes as to elements utilized which can be linear or parabolic.

The code has been checked against theoretical and experimental results as well proving its reliability.

1. Introduction

In the evolution of fracture mechanics approach to pressure vessel integrity analysis, growing importance has been given to crack arrest properties experienced by structural materials.

Whether or not the crack arrest toughness, K_a, is a material property such as K_c, it is clear that it is going to play an important role in fracture prevention since it eventually releases designer from ruling out unstable crack propagation in any condition, including accident conditions, in as long as the crack will arrest without jeopardizing the pressure retention capability of the structure.

This has led ENEA-DISP to investigate the arresting capabilities of steels in general and low alloy carbon steel in particular either from analytical and experimental point of view.

The purpose of this paper is to present the approach to the crack arrest problem which has been developed at CISE under ENEA-TERM contract and ENEA-DISP technical responsibility

The first goal in the ENEA crack arrest program which this paper is referring to has resulted in the preparation of the finite elements computer program SPACCA /1, 2/ (Simulazione di Propagazione e Arresto di Cricche in Condizioni di Accelerazione qualunque) based on linear elastic fracture mechanics.

The code analyzes Mode I crack propagation in two dimensions. Phase II of the program, scheduled to start in 1985, will extend SPACCA into elastic-plastic domain. Code predictions, already compared with theoretical solutions, will also be checked against instrumented CCA specimens behaviour in 1985.

2. Theoretical approach

Looking at the problem of dynamic crack propagation from an energy balance stand point, it can be said that as crack initiation takes place when the applied energy release rate G equals a critical value G_c, characteristic of the material, so propagation is maintained in as long as the applied G(t) matches dynamic energy release rate G (å) (see Nilsson and Brickstad /3/) which has been found to be a function of crack speed, å, for most materials:

$$G(t) = G_D(\dot{a}) \tag{1}$$

Conversely, arrest occurs any time G (t) drops below the minimum value experienced by $G_D(\dot{a})$. Eq. (1) implies the knowledge of either the $G_D(\dot{a})$ function to derive the crack propagation velocity and, eventually, the arrest stage or the time history of crack propagation to infer the $G_D(\dot{a})$ function. This two approaches are referred to as inverse and direct problem respectively.

In both cases, anyway, it must be given the law of stress relaxation at the crack tip as the flaw is running across the material.

SPACCA code is using a nodal relaxation technique (see Brickstad and Nilsson /4/) which relates the nodal reaction F to the crack tip mesh spacing Δ according to the following equation:

$$F=F_0\left(1 - \frac{\Delta a}{\Delta}\right)^{\alpha} \tag{2}$$

where F_0 is the nodal force at the time in which relaxation starts, Δa the crack length increment and α a parameter the rate at which the relaxation F/F_0 depends on, α=1 for simplified version of the Keegstra (KK) model /5/, α>1 for Rydholm , Fredriksson,Nilsson (RFN) model /6/ and α<1 for Malluck, King (MK) model /7/.

Once stress distribution is known the applied G(t) can be inferred from energy considerations (see Kanninen /8/) or calculated using path integrals (see Ahmad et al. /9/, Kishimoto et al. /10/, Nishioka and Atluri /11/).

3. Numerical integration of motion equation

Since dumping effects have been disregarded the equation of motion considered is the following:

$$M\ddot{U}+KU=f(t) \tag{3}$$

with the initial conditions:

$$KU_0=f(0);\ \dot{U}_0=0 \tag{4}$$

Equation (3) has been solved using the following explicit scheme:

$$\begin{aligned} U_{n+1} &= U_n + h\dot{U}_n + \frac{h^2}{2}\ddot{U}_n \\ \dot{U}_{n+1} &= \dot{U}_n + h\,\frac{\ddot{U}_n + \ddot{U}_{n+1}}{2} \\ L\ddot{U}_{n+1} &= f_{n+1} - KU_{n+1} \end{aligned} \tag{5}$$

where L is the lumped mass matrix.

Eq. (5) derives from a more general class of integration scheme proposed by Newmark (see Bathe /12/). It has a stability limit of $h=T_{min}/\pi$, where T_{min} is the lowest period of the

structure discretized. Its accuracy is of the 3rd order.

The SPACCA code has the option to use a class of inplicit integrators, with consistent mass matrix, including either the Euler back scheme and the trapezia one; both are unconditionately stable with accuracy of the 2nd and 3rd order respectively.

Computer usage convenience suggests the use of the explicit scheme, eq.(5), for both the direct and inverse problem of dynamic crack propagation.

4. Direct problem solutions

Code's reliability has been checked against some analytical solutions available in the literature.

Two cases have been considered. The first was referring to a plate subjected to an uniaxial stress state σ_0 with a crack starting from zero length and running with constant velocity on a plane perpendicular to the stress direction. Until reflected stress waves do not reenter the process zone, i.e. in the early stage, the problem can be considered equivalent to one of the cases already treated by Broberg /13,14/ and directly compared.

In order to have a comprehensive knowledge of the code's performances several meshes and different relaxation models,eq.(2),have been considered.

As to the mesh two schemes were used: the first employed 400 square linear elements, 441 nodes and 840 degrees of freedom, the second 100 square parabolic elements with 341 nodes and 662 degrees of freedom.

Each of the two meshes have been used to analyze the three relaxation models: the KK, the RFN and the MK model.

Plain strain conditions were considered in the computation. Input data are shown in Table I. Figures 1 and 2 depict adimensional stress intensity factors versus crack length normalized to the plate half width L, for linear and parabolic elements respectively. Also shown is the Broberg analytical solution (solid line). The agreement between the theoretical solution and those computed by SPACCA code, already good for linear elements, is further improved making use of the parabolic ones.

The second problem considered is the Baker case of a semi-infinite crack subjected to a stress wave /15/. Again it was assumed a constant propagation speed upon arrival of the stress wave produced by the application of a stress state σ_0 on the border of plate. The initial crack lenght was 0.4L. Input data are shown in Table I.
Figure 3 is a plot of numerical results obtained for the three relaxation models compared with the theoretical result (solid line).

At last two different tests performed by Kalthoff et al. /16/ have been checked.
Figure 4 shows the DCB specimen considered by Kalthoff and the mesh used in the SPACCA code. Dimensions and characteristic of the material are listed in Table II. For the tests considered the experimental trend of crack speed was available, as shown in figure 5.The velocity profiles actually measured were relative only to the shelf of figure 5. They have been completed to provide input data to the code by assuming a linear trend during both initial acceleration and final deceleration.

Figure 6 is a plot of numerical results and Kalthoff solution (solid line) in terms of K_D versus crack length, a, for the two velocity profiles of figure 5 which refer to two distinct displacements given on the load line of the specimens and hence to two different static K_0 of 2.32 MPa $\sqrt{m}$ and 1.33 MPa $\sqrt{m}$, respectively.

5. Inverse problem solutions

Again the Kalthoff tests have been used, this time considering as input datum the K_D characteristic of the material /16/.

Figure 7 is a plot of SPACCA code results compared always to the Kalthoff solution (solid line). For these cases velocity profiles are calculated by the code. They are plotted in figure 8 against the experimental ones of figure 5.

6. Conclusions

The SPACCA computer code has been used against theoretical and experimental cases available in the literature. The agreement between numerical solutions and theoretical or experimental ones is excellent. All the relaxation models used (KK, RFN and MK) seem to yield almost equally reliable results.

Parabolic elements provide greater accuracy than the linear ones.

The Code will be extended into the elastic-plastic domain.

REFERENCES

/ 1 / A. Cella, C. Lusso, C. Sampietri - Studio della propagazione dinamica di cricche in strutture elastiche bidimensionali: il programma BICVI. CISE 2257, 1983

/ 2 / C. Lusso, C. Sampietri - Studio della propagazione dinamica di cricche in strutture elastiche bidimensionali: i programmi BICVI e BICRIC . CISE 2451, 1984

/ 3 / F. Nilsson, B. Brickstad - Dynamic Fracture Mechanics, rapid crack growth in linear and non-linear materials. Advanced Seminar on Fracture Mechanics, 1983

/ 4 / B. Brickstad, F. Nilsson - Explicit Time Integration in FEM-Analysis of Dynamic Crack Propagation, Numerical Methods in Fracture Mechanics, 1980

/ 5 / P.N.R. Keegstra, J.L. Mead, C.E. Turner - A two-dimensional Dynamic linear-elastic finite-element program for the analysis of unstable crack propagation and arrest. Numerical Methods in Fracture Mechanics, 1978

/ 6 / G. Rydholm, B. Fredriksson, F. Nilsson - Numerical investigation of rapid crack propagation. Numerical Methods in Fracture Mechanics, 1978

/ 7 / J.F. Malluck, W.W. King - Fast fracture simulated by a finite-element analysis which accounts for crack-tip energy dissipation. Numerical methods in fracture mechanics, 1978

/ 8 / M.F. Kanninen - A critical appraisal on solution techniques in dynamic fracture mechanics. Numerical Methods in Fracture Mechanics, 1978

/ 9 / J. Ahmad, J.Jung, C.R. Burnes, M.F. Kanninen - Elastic-plastic finite element analysis of dynamic fracture, Engineering Fracture Mechanics, 1983

/ 10 / K. Kishimoto, S. Aoki, M. Sakata - Dynamic stress intensity factors using J-integral and finite element method. Engineering Fracture Mechanics, 1980

/ 11 / T.Nishioka, S.N. Atluri - A numerical study of the use of path indipendent integrals in elasto-dynamic crack propagation. Engineering Fracture Mechanics, 1983

/ 12 / K.J. Bathe - Finite Element procedure in engineering analysis. Prentice Hall, Englewood Cliffs, N.J., 1982

/ 13 / K.B. Broberg - The propagation of a brittle crack. Arkiv för Fysik, 1960

/ 14 / K.B. Broberg - On the speed of a brittle crack, Journal of applied mechanics, 1964

/ 15 / B.R. Baker - Dynamic stress created by a moving crack. Journal of applied mechanics, 1962

/16 / J.F. Kalthoff, J. Beinert, S. Winkler - Measurements of dynamic stress intensity factors for fast running and arresting cracks in double-cantilever-beam specimens. Fast Fracture and crack arrest, ASTM STP 627, 1977.

Table I - Input data for both Broberg's and Baker's cases

Density	$\rho=8.10^3 kg/m^3$
Elastic Modulus	$E=2.067\ 10^{11} Pa$
Poisson's Ratio	$\nu=1/3$
Longitudinal Wave Velocity	$c_1=6225$ m/s
Shear Wave Velocity	$c_2=3112.5$ m/s
Crack Velocity	$\dot{a}=1556.25$ m/s
Quarter-Plate Size	L=2.4m
Uniform Load	$\sigma_0=1Pa$
Critical Integration Time-Step	13 μs (linear elements)
	12 μs (parabolic)

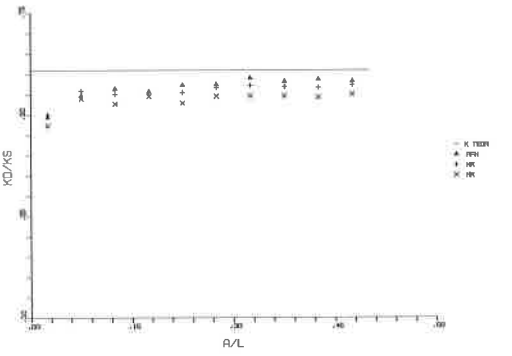

Fig. 1 - Broberg's case. Linear elements
Normalized stress intensity factor

Table II - Input data for both direct and inverse Kalthoff's case

Specimen's Height	2H=0.127 m
Specimen's Length	L =0.321 m
Specimen's Thickness	s =0.010 m
Initial Crack Lenght	$a_0=0.068$ m
Material	Araldite B
Density	$\rho=1226.25\ kg/m^3$
Elastic Modulus	$E=3.66\ 10^9 Pa$
Poisson's Ratio	$\nu=0.392$
Critical Integration Time-Step	0.7μs(parabolic elements)

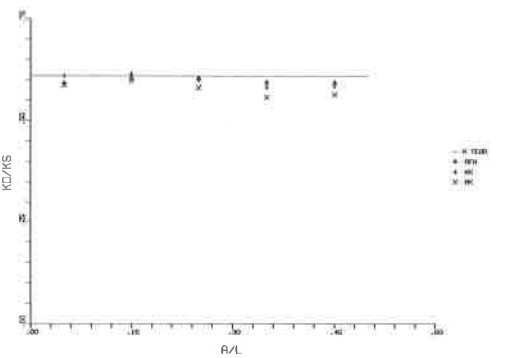

Fig. 2 - Broberg's case. Parabolic elements
Normalized stress intensity factor

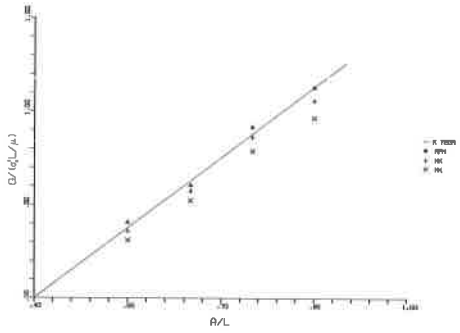

Fig. 3 - Baker's case. Parabolic elements
Normalized energy release rate

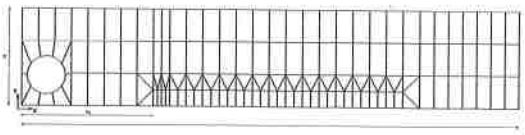

Fig. 4 - Kalthoff's DCB specimen .
Finite element idealization

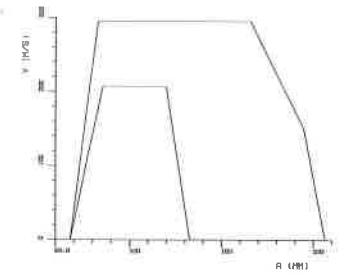

Fig. 5 - Kalthoff's DCB specimen .
Crack tip velocity profile

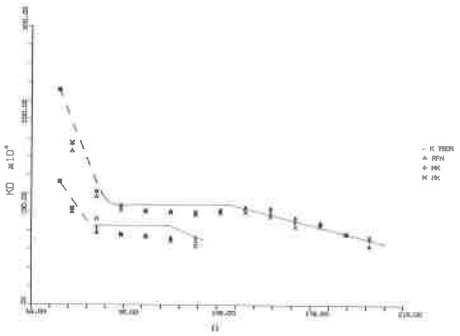

Fig. 6 - Kalthoff's DCB specimen.
Stress intensity factor
(direct problem)

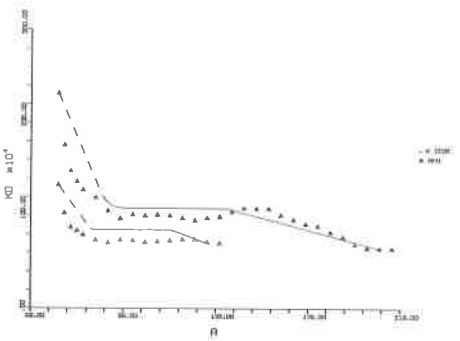

Fig. 7 - Kalthoff's DCB specimen.
Stress intensity factor
(inverse problem)

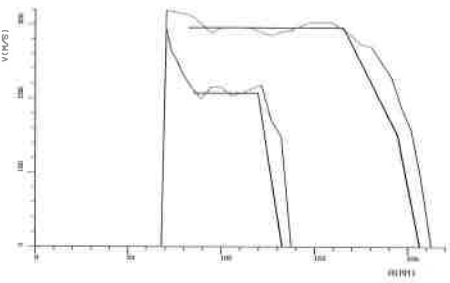

Fig. 8 - Kalthoff's DCB specimen.
Crack tip velocity (experimental
and calculated)